Propagation of classical waves in random media

C. M. Soukoulis and S. Datta

Ames Laboratory and Department of Physics and Astronomy,
Iowa State University, Ames, Iowa 50011

E. N. Economou

Research Center of Crete/FORTH and Department of Physics
University of Crete, Heraklio, Crete, Greece

An extension of the well-known coherent-potential-approximation is developed for the study of various properties of random arrangements of spherical dielectric scatterers. Some of the short-range order is taken into account by considering a coated sphere as the basic scattering unit. A generalization of the energy-transport velocity is obtained. The validity of our approach is checked by comparison with experimental results, as well as with numerical calculations. Results for the long-wavelength effective dielectric constant, phase velocity, energy-transport velocity, mean free path, and diffusion coefficient are presented and compared with experiments on scattering from dielectric spheres. In addition, our findings suggest that the positions of the band gaps in periodic dielectric structures are closely related with the range of localized states in random dielectric media.

I. INTRODUCTION

In recent years, there has been growing interest in studies of the propagation of classical waves in random media.[1] While some of the features associated with weak localization, such as enhanced coherent backscattering, have been detected in light scattering experiments,[1] the localization of electromagnetic waves or other classical waves in random systems has not been established beyond doubt. It is well known[1-3] that it is harder to localize classical waves, mainly due to the fact that at low frequency the effect of disorder tends to be wiped out for classical waves due to an ω^2 factor, whereas electrons at low energy are trapped more effectively, even by a weak random potential. It has been suggested[2,3] that an intermediate-frequency window (or windows) of localized states separates the low-frequency extended states characterized by Rayleigh scattering from the high-frequency extended states described by geometric optics. Theories based on the weak scattering limit and on the coherent-potential approximation (CPA) predict frequency intervals within which localization should be observed.[1,3-6] These predictions are based on approximations which are uncontrollable; in Ref. 3, results based on a reliable numerical technique provide evidence supporting the existence of spectral regions of localized eigenstates, at least for scalar classical waves. However, there is no conclusive experimental evidence yet, although experiments by Genack and collaborators[7] provide some indications that light localization is possible. In addition, it was recently recognized[8] that considerable care is needed in interpreting low values of the diffusion coefficient in studies for the search of light localization. In particular, the Amsterdam group[8] presented experimental results for the diffusion coefficient D and the transport mean free path

ℓ_t. We want to stress that ℓ_t is the transport mean free path, which is defined as the length over which momentum transfer becomes uncorrelated. This is different from the scattering mean free path ℓ which describes the decay length of the single-particle Green's function and is easily calculated within the CPA. The transport mean free path involves an extra factor $(1 - \cos\theta)$ in the calculation of the total cross section. Here we have assumed that $\ell \approx \ell_t$, and some preliminary results tend to confirm that ℓ and ℓ_t are not much different from each other. In any case, the Amsterdam group's results demonstrated that in the strongly scattering random dielectric medium, the low values of the diffusion coefficient $D = v_E \ell_t / 3$ were caused by extremely small values of the transport velocity, v_E, and not by the small values of ℓ_t, which signify strong localization. It is, therefore, possible that in a random medium the transport velocity can be much lower than the phase velocity, which is approximately equal to the velocity of light, c, divided by an appropriate average index of refraction. To explain this discrepancy, the Amsterdam group[8] presented a treatment of the transport velocity based on the low-density approximation of the Bethe-Salpeter equation. They argued that their approach confirmed the observed smallness of the transport velocity. However, Barabanenkov and Ozrin,[9] as well as Kroha et al.,[10] also developed a theory based on the low-density approximation of the Bethe-Salpeter equation, with a generalized Ward identity for scalar waves. Their conclusion was that the expression for the transport velocity was renormalized in the same way as the phase velocity. Thus, the question of the proper transport velocity, especially at high concentration of scatterers, remains open. In the present work we develop a generalization of the well-known CPA, which combined with the Amsterdam group approach produces results in reason-

able agreement with the experimental observations.

The difficulty in localizing classical waves has led to suggestions of alternative pathways to localization. John[2] has proposed that classical localization may be more easily achieved for a weakly disordered system of almost periodically arranged dielectric structures in the frequency regime near a band gap. We can very reliably calculate the bands and gaps if the dielectric spheres form a periodic lattice. It is very plausible that a connection between the gaps in periodic systems and the ranges of localized states in a random system exist,[11] at least for weak disorder and/or for a high concentration of dielectric spheres (approaching the close-packing limit). Indeed, in this case the regions of localized states (being at the tails inside the gaps) practically coincide with the positions of the gaps. It will be very interesting to check if the theoretical approximate approaches, even on the level of a generalized CPA, reproduce the above prediction as we move near the close-packing limit.

In this paper, we present a simple approach that is based on an extension of the Amsterdam group method and on a generalization of the well-known CPA, appropriate for the case of high dielectric constant identical spheres placed randomly in a host of low dielectric constant. We take into account the short-range order induced by the spherical shape of the scatterers by considering a coated sphere as a scattering unit. The host coating thickness decreases as the concentration of the dielectric spheres increases. To calculate the macroscopic properties of the random system, the coated sphere is embedded in an effective medium with an effective dielectric constant, ϵ_e. The quantity ϵ_e is self-consistently determined by demanding that the average forward-scattering amplitude $f(0)$ is equal to zero. Once the quantity ϵ_e is determined, an effective propagation constant $q \equiv (\epsilon_e)^{1/2}\omega/c$ is defined, where c is the velocity of light, and, therefore, one can immediately find the mean free path $\ell=0.5/\mathrm{Im}(q)$, the renormalized wave vector $k = \mathrm{Re}(q)$, and other effective macroscopic properties of the random system. The validity of this approach is verified by comparison with experimental results, as well as with numerical calculations. The coated CPA results for the mean free path, phase velocity, and diffusion coefficient are in reasonable agreement with experiments. We want to caution the reader that the phase velocity obtained from our newly developed coated CPA does not, in general, coincide with the energy-transport velocity. Our CPA calculates the average Green's function $\langle G \rangle$ and not $\langle GG \rangle$ which is related with transport properties. However, there is no reliable transport theory for $\langle GG \rangle$ in the high concentration limit, where most of the experiments are done. For lack of any better theories, in the present paper we have developed a combination of the coated CPA with the energy-transport theory of Lagendijk et al.[8] This new theory reduces to that of Lagendijk et al.[8] in low concentration and seems to be consistent with experiment in high concentration. The mobility edge trajectory which is obtained by employing the potential well analogy[12] (PWA) together with the coated CPA,[12] agrees reasonably well with the positions of the band gaps in the periodic dielectric structures, in spite of

the fact that the comparison is made for high concentration where our CPA is less accurate. In addition, different definitions of the velocity of light in random media will be introduced, and compared with experiments. The energy-transport velocity introduced by the Amsterdam group,[8] the effective phase velocity derived by the coated CPA, the phase velocity derived[4] from the Green's function and the energy velocity based on the combination of coated CPA and the Amsterdam group method will be compared with each other and with experiment.

II. MODEL AND METHODS OF CALCULATIONS

For our studies we consider a composite medium consisting of two lossless materials, with dielectric constants ϵ_1 and ϵ_2. Our composite medium is assumed to consist of spheres with diameter, $d = 2R$ and dielectric constant ϵ_2 randomly placed within the host material with dielectric constant ϵ_1. We will only consider cases where ϵ_1 and ϵ_2 are real and positive, i.e., cases where there is no absorption and free propagation exists for each of the two components. The random medium is characterized also by f, the volume fraction occupied by the spheres and, of course, the ratio $\mu = \epsilon_2/\epsilon_1$ of the two dielectric constants. We take $\epsilon_2 > \epsilon_1$ and nonoverlapping spheres (except in Fig. 1, where we show also results for the case of $\epsilon_1 > \epsilon_2$ and overlapping spheres). It should be emphasized that the shape of the scatterers (e.g., sphere vs cube) may play an important role. The spheres do not form an infinitely connected channel even for the high volume fraction f, while a completely random mixture of cubes (or another flat surface shape) may easily form an infinitely connected channel. It must be pointed out that it is the persistence of the dominant role of the single scatterer even for high f that makes our CPA approach more reliable.

We consider first the propagation of classical waves in a random medium described by the wave equation for the scalar field ψ:

$$\nabla^2\psi - \frac{\epsilon(\mathbf{r})}{c^2}\frac{\partial^2\psi}{\partial t^2} = 0 \qquad (1a)$$

or

$$\nabla^2\psi + \frac{\omega^2}{c^2}\epsilon(\mathbf{r})\psi = 0. \qquad (1b)$$

The corresponding equations for the electronic case are

$$\nabla^2\psi - \frac{2m}{\hbar^2}V(\mathbf{r})\psi + \frac{2mi}{\hbar}\frac{\partial\psi}{\partial t} = 0, \qquad (2a)$$

$$\nabla^2\psi + \frac{2m}{\hbar^2}[E - V(\mathbf{r})]\psi = 0. \qquad (2b)$$

In the time domain, the electronic [Eq. (2a)] and the classical wave [Eq. (1a)] equations are not equivalent; as a result, time dependent processes such as the diffusion of an initially localized pulse cannot be carried

over from the electronic to the classical wave case without further analysis.[8-10] On the other hand, in the frequency domain the two equations [Eqs. (1b) and (2b)] are equivalent.[3] Since $\epsilon(\mathbf{r})$ is positive definite and $\omega^2 \geq 0$, it follows immediately that $E \geq V_{max}$ for the corresponding
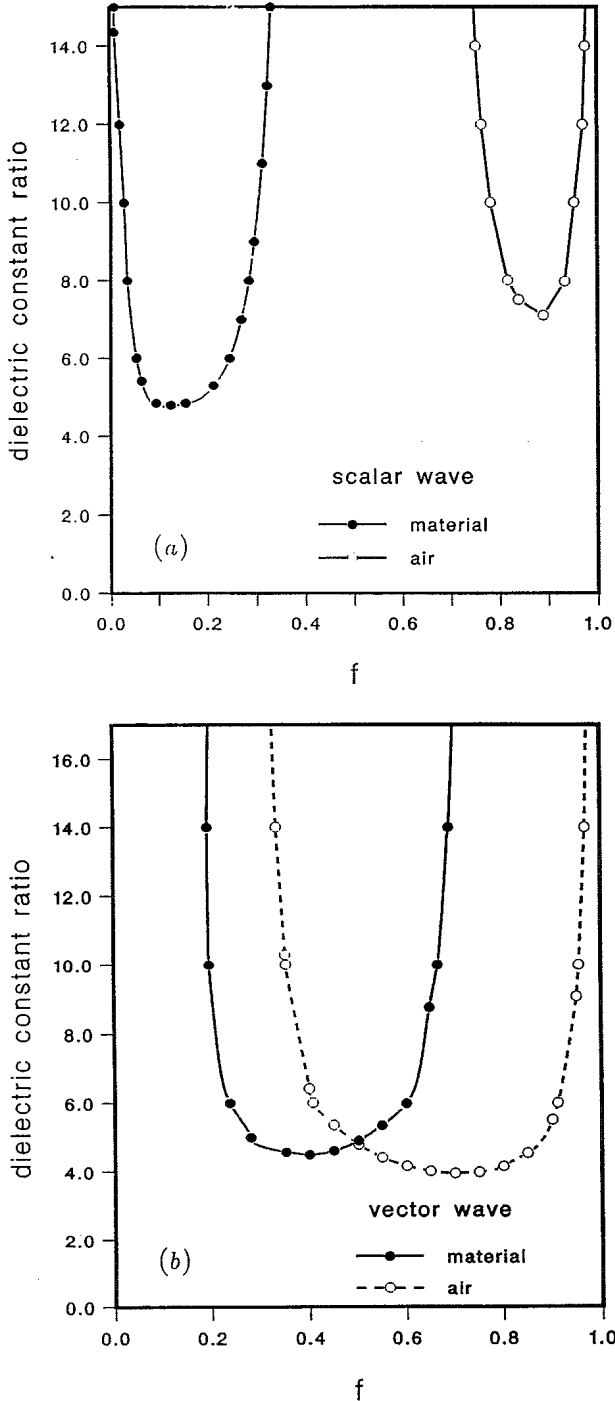

FIG. 1. The threshold value of the dielectric constant ratio $\mu = \epsilon_2/\epsilon_1$ for the opening of the first band gap is plotted as a function of the filling ratio f of dielectric spheres arranged in a diamond lattice. The dielectric constant of the spheres is ϵ_2 and the host ϵ_1 (material case) or vice versa (air case of overlapping spheres). The (a) case is for scalar waves, while (b) is for electromagnetic waves.

electronic problem. This means that the classical wave problem is mapped onto the electronic problem for an energy larger than the maximum value of the potential. The gaps in the classical wave problem are equivalent to gaps for $E \geq V_{max}$, i.e., in the classically unbounded regime for the electronic problem. The existence of gaps in this region of energy for three-dimensional (3D) periodic systems is not *a priori* guaranteed. As a matter of fact, only under rather extreme conditions, gaps above V_{max} appear.[3,13,14] In Fig. 1(a), we plot the threshold value of the dielectric constant ratio $\mu = \epsilon_2/\epsilon_1$ for the creation of a gap for the diamond lattice, as a function of the filling ratio f. Notice that for very small values of f and large values of f, no gap exists for any value of the dielectric constant ratio. In Fig. 1(b), we plot the results of the threshold values of μ vs f, for the case of electromagnetic (EM) waves and again for the diamond lattice. Notice that in the EM wave case, the optimum f is around 0.40, higher than the f of the classical case [see Fig. 1(a)] which is 0.15. The corresponding minimum values of μ are very close to 4 for both cases.

The theory of wave propagation in a 3D weakly random medium is based on the implicit assumption that disorder modifies the phase of the unperturbed wave function. The periodic wave vector k_0 is renormalized to k and at the same time gains an imaginary part $i/2\ell$, where ℓ is the phase coherence length or scattering mean free path, i.e., $k_0 \to k + i/2\ell$. As long as $k\ell \gg 1$, the effect of disorder on the amplitude of the unperturbed wave function is negligible, thus justifying the traditional approach which ignores any amplitude fluctuations. However, as the disorder becomes stronger, i.e., as $k\ell$ approaches unity, amplitude fluctuations of ever increasing magnitude and extent, start developing. As we enter the localized region, the wave still has large amplitude fluctuations but, in addition, its amplitude decays exponentially on the average for large distances as exp $[-r/\lambda]$, thus defining the localization length λ. Many versions of an approximate theory have been developed which express the amplitude related quantities, with phase-related quantities k and ℓ. Probably the most accurate among them is the so-called potential well analogy (PWA),[12] which connects the self-consistent theory of localization to the problem of finding a bound state in a potential well. For example, the amplitude fluctuations of the wave function in the random system correspond to the scattering length of the scattering solution and the localization length corresponds to the decay length of the bound solution in the potential well. So the approximate PWA technique requires as inputs the renormalized wave vector k and the mean free path ℓ. A very efficient way to obtain both k and ℓ is the so-called coherent-potential approximation (CPA). The CPA introduces a yet undetermined effective medium, characterized by an effective complex frequency-dependent dielectric constant ϵ_e or equivalently an effective propagation constant q, such that

$$q = \left(\frac{\omega^2}{c^2}\epsilon_e\right)^{1/2} = k + i/2\ell \qquad (3)$$

the quantity q (or ϵ_e) is determined by the condition that the resulting scattering, when a spherical region

of the effective medium is replaced by the true random medium, be equal to zero on the average. To implement this general idea, we consider the homogeneous effective medium (dotted region in Fig. 2) as made up of identical nonoverlapping, space filling Wigner-Seitz cells of fcc structure. The volume of each cell equals $V_p = z^3 V$, where $V = 4\pi R^3/3$ is the volume of the sphere of the high dielectric material presented as a black sphere in Fig. 2 (R is taken as the unit of length). Within each cell, we take into account two scattering configurations as shown in Fig. 2. The first one consists of a black sphere placed at the center of the cell and is surrounded by a spherical region of low dielectric material (white region in Fig. 2). The outer radius is R_s and the volume of the coating is $V_s - V$. This white coating takes into account approximately the fact that as a result of the spherical shape of the scatterers there is host material around each black sphere even at very high volume fractions (i.e., for $f \leq 0.6$). The other configuration simulates the case where at the center of the cell is the host material surrounded by the neighboring black spheres; for simplicity the rather irregular shape of this piece of host material is replaced by a sphere of radius R_v and volume V_v. The probability of each configuration and the radii R_s and R_v depend on f and on z. In previous studies[3,4,12] we and other authors have considered as basic scattering units a black sphere with probability f and a white sphere of equal radius with probability $1 - f$. This previous choice, which treats the black and white regions equally, neglects the basic topological and geometrical difference between the spheres and the host material. In particular

for high f, the white sphere is not only less probable but its radius is smaller than the radius of the black sphere. Obviously the coated solid sphere, as well as the white sphere with a different radius, approximates much better the real random system of dielectric spheres. To calculate the effective dielectric constant ϵ_e or the effective propagation constant q, we require that $\langle f(0) \rangle = 0$, where $\langle f(0) \rangle$ is the average forward-scattering amplitude. In particular, for the coated CPA we must satisfy the following condition:

$$p_1 f_1(0) + p_2 f_2(0) = 0, \qquad (4)$$

where p_1 and $f_1(0)$ are the probability and the forward-scattering amplitude of the first configuration of a single-coated sphere embedded in the effective medium with dielectric constant ϵ_e; p_2 and $f_2(0)$ are the corresponding quantities for the white sphere (host material) as the basic scattering unit. We must determine the quantities p_1, p_2, R_s, R_v, and z. Obviously $p_1 V$ is proportional to f, $p_1 (V_s - V) + p_2 V_v$ is proportional to $1 - f$ (with the same proportionality constant), and $p_1 + p_2 = 1$. Thus $p_1 = f\bar{V}/V$, $p_2 = (1 - fV_s/V)\bar{V}/V_v$, where $\bar{V} = p_1 V_s + p_2 V_v$ and $\frac{p_2}{p_1} = \frac{V - fV_s}{V_v f}$. The volume V_s can be taken as equal to $V_p/(n' + 1)$, where n' is the average number of black spheres within the volume V_p around the central one. The quantity n' is proportional to f and to the available volume $V_p - V$, i.e., $n' = af(z^3 - 1)$. The proportionality constant, a, can be determined by the requirement that in the close-packed limit ($f = 0.74$) and for $z = 3$, $n' \approx 12$. Such a requirement leads to a value of a less than unity, which does not guarantee that $p_2 > 0$. To avoid this problem, we chose $a = 1$; thus, the resulting expression for V_s is $V_s = Vz^3/[f(z^3 - 1) + 1]$. The quantity V_v can be taken equal to $V_p - n''V_s$, where n'', the average number of spheres within the volume V_p, is proportional to the available volume V_p/V and to the volume fraction f with the proportionality constant taken, as before, equal to one. Thus, $V_v = z^3(V - fV_s)$. With the choices we have made, the result depends on the free parameter z. We fixed the value of z by fitting our results to the $f \to 0$ case for which exact results are available. We found that $z = 1.65$ reproduced very accurately the exact results for all frequencies we tested. In Fig. 3, we plot the radius R_s of the coated sphere and the radius R_v of the host sphere vs the volume fraction f of the high dielectric material. Notice that as $f \to 0$, R_s, as well as R_v, approach the value of zR, where R is the radius of the high dielectric constant sphere, which is taken to be equal to one. As f approaches the fcc close packing of 74%, we have that $R_s = 1.078R$ and $R_v = 0.688R$, which are close to the corresponding values $R_s = 1.086R$ and $R_v = 0.414R$ of the close-packed fcc lattice. This is one requirement we had to satisfy, and the choice of $z = 1.65$ gave a reasonable agreement. As we mentioned before in Eq. (4), $f_1(0)$ and $f_2(0)$ are the forward-scattering amplitude of the coated solid sphere and of the host sphere, respectively. The forward-scattering amplitude of either a coated sphere or a host sphere is given by
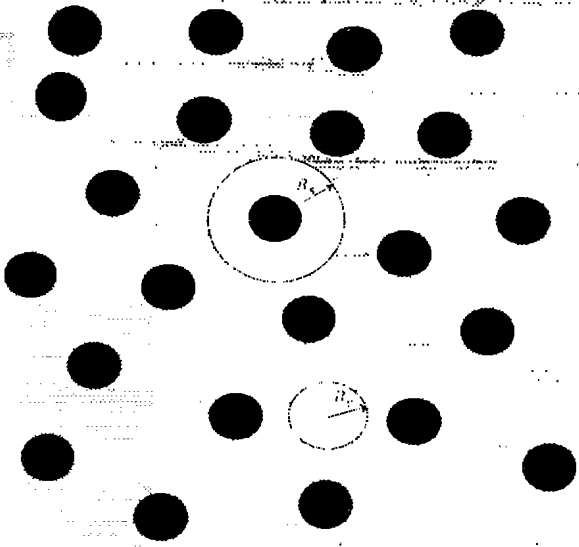

FIG. 2. A typical configuration of the random system. The solid spheres of radius $R = 1$, are the scattering centers, their volume fraction is f. There are two types of scattering units, a coated black sphere of radius $R_S > R$ and a host material sphere of radius R_v. The dotted region is the effective medium with a yet undetermined dielectric constant.
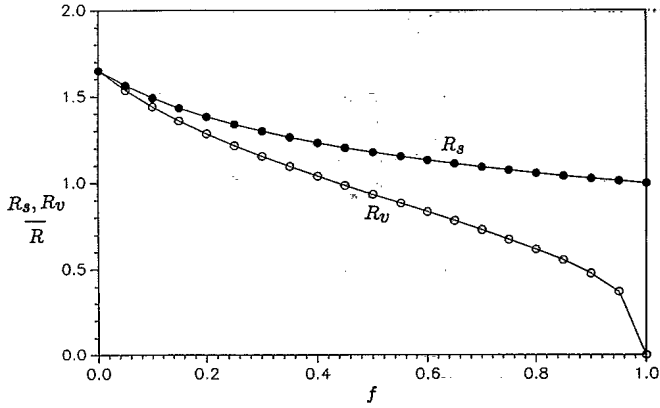
$$f(0) = \frac{i}{2q} \sum_{\ell=1}^{\infty} (2\ell + 1)(a_\ell + b_\ell), \qquad (5)$$

FIG. 3. The dependence of the radius R_s and R_v on the filling ratio f.

where $q = \frac{\omega}{c}\sqrt{\epsilon}$ is the wave vector in the effective medium and a_ℓ and b_ℓ are given in Ref. 15 for both the coated sphere as well as the single sphere. In addition, the self-energy Σ is given (to first order in the concentration) by

$$\Sigma = -4\pi n f(0), \tag{6}$$

where n is the number density (i.e., concentration) of the particular type of scatterer. In addition, we also have that the total scattering cross section σ is equal to

$$\sigma = 4\pi \mathrm{Im} f(0)/q = -\mathrm{Im}\Sigma/q\, n. \tag{7}$$

Before we discuss the solution of the coated CPA [Eq. (4)], we want to make some comments concerning results that one can obtain in the low concentration limit. Usually perturbation theory is inadequate in the region of strong scattering. The standard way to go beyond perturbation theory is to treat each scattering center independently of all the others and then simply add the effects (complete omission of the multiscattering processes). Under this assumption, the scattering mean free path ℓ is given by

$$\ell = 1/n\sigma = -q/\mathrm{Im}\Sigma, \tag{8}$$

where ℓ is given in units of the radius R of the scattering sphere. In addition, the phase velocity is given[4,8] by

$$v_{\mathrm{ph}} = c\sqrt{1 + \mathrm{Re}\Sigma/q^2}, \tag{9a}$$

which for small values of $\mathrm{Re}\Sigma/q^2$ can be written as

$$v_{\mathrm{ph}} = \frac{c}{\sqrt{1 - \mathrm{Re}\Sigma/q^2}}. \tag{9b}$$

Recently, the Amsterdam group[8] has suggested that the correct transport velocity that must enter into the diffusion equation is the energy-transport velocity, v_E. The expression for v_E is given by Eqs. (28) and (29) in Ref. 8. The important point made by them is that v_E is always less than the velocity of light, which is not true for either the phase velocity or the group velocity, especially close

to the Mie resonances of a finite single scatterer. We will later present results for both v_{ph} and v_E, together with the effective velocities obtained from the new developed coated CPA.

III. RESULTS AND DISCUSSION

To solve Eq. (4), i.e., the equation $\langle f(0) \rangle = 0$ or equivalently $\langle \Sigma \rangle = 0$, we transform it into an iterative equation of the form $q_{n+1} = q_n + A\langle \Sigma \rangle$, where n is the order of iteration and A is chosen using the weak scattering limit and demanding as good a convergence as possible. We have used $A = -3/8\pi q_n$. After a successful convergence of q, which implies $\langle f(0) \rangle = 0$ or $\langle \Sigma \rangle = 0$, the mean free path $\ell=0.5/\mathrm{Im}(q)$, the renormalization wave vector $k =\mathrm{Re}(q)$, the dimensionless localization parameter $k\ell$, and the effective phase velocity $v = \omega/k$ are determined. In the PWA formalism[12] there is a mobility edge, separating extended states from localized states when $k\ell \simeq 0.84$. As mentioned before, the free parameter z in our coated CPA theory was chosen in such a way that our coated CPA gives the same value of the mean free path ℓ as the weak scattering expression given by Eq. (8) for very low values of f. Indeed, the choice of $z = 1.65$ in the coated CPA gave mean free paths in excellent agreement with the weak scattering expression, for different values of the incident frequency. In addition, the choice of $z = 1.65$ gave excellent agreement (between the coated CPA results and the band structure results) for the long-wavelength effective dielectric constant ϵ_e for all values of f. This is clearly shown in Fig. 4 where we plot the long-wavelength effective dielectric constant vs the filling ratio f for the band structure results[16] of an fcc lattice of dielectric spheres of dielectric constant of 13 embedded in a medium with the dielectric constant equal to one. Notice that our coated CPA results (solid
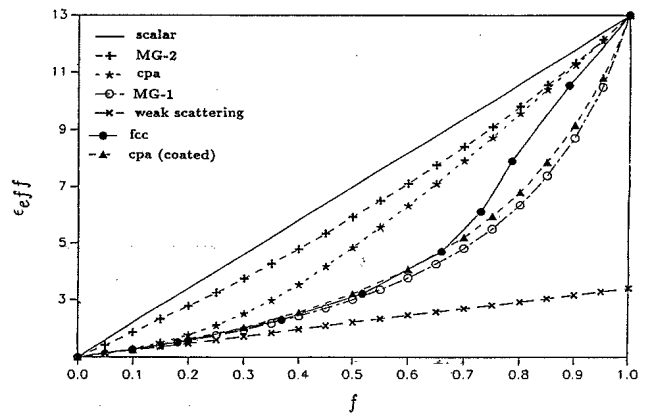

FIG. 4. The long-wavelength dielectric constant ϵ_e for a sphere with dielectric constant $\epsilon =13$ in a host of $\epsilon_1 = 1$ as a function of the sphere filling ratio f. Results of the newly developed coated CPA are compared with the Maxwell-Garnett (MG-1), scalar, conventional CPA, and weak scattering results as well as numerical data based on periodic fcc structures. MG-2 is the Maxwell-Garnett approach for spheres of dielectric constant $\epsilon_2 = 1$ in a host of $\epsilon_1 = 13$.

triangles) agree extremely well with the very accurate fcc results (solid circles) all the way to $f \simeq 0.74$, which is the close-packing concentration. This is impressive, because the coated CPA is expected to be inaccurate for $f > 0.64$ (the random close-packed limit) and completely inapplicable for $f > 0.74$ (the fcc close-packed limit). Our coated CPA results are in reasonably good agreement with the Maxwell-Garnett theory which is given by

$$\epsilon_e = \epsilon_1 \left(\frac{2\epsilon_1 + \epsilon_2 + 2f(\epsilon_2 - \epsilon_1)}{2\epsilon_1 + \epsilon_2 - f(\epsilon_2 - \epsilon_1)} \right), \tag{10}$$

where ϵ_1 is the dielectric constant of the background and ϵ_2 is the dielectric constant of the spherical scattering centers. In Fig. 4, the Maxwell-Garnett theory (MG-1, white circles) denotes the case where $\epsilon_1 = 1$, $\epsilon_2 = 13$, and f is the concentration of the ϵ_2 material. Just for comparison, we also present in Fig. 4 the Maxwell-Garnett theory (MG-2, crosses) of $\epsilon_2 = 1$ and $\epsilon_1 = 13$ with f now the concentration of the ϵ_1 material. Only for high values of f does the MG-2 theory agree with the fcc numerical results. In Fig. 4 we also present the results of the scalar theory, where $\epsilon_e = f\epsilon_2 + (1 - f)\epsilon_1$, with $\epsilon_1 = 1$ and $\epsilon_2 = 13$, which is much higher than the numerical results and all the other theories. In order to reinforce the point that the coated CPA is a substantial improvement over the weak scattering limit or previous CPA's,[3,4,12] where the geometry was not treated properly, we have also plotted in Fig. 4 results for ϵ_e within the weak scattering limit ($\times$), and within the conventional CPA (star). The long-wavelength limit for the effective dielectric constant in the weak scattering limit is given by

$$\epsilon_e = \epsilon_1 + 3f \left(\frac{\epsilon_2 - \epsilon_1}{\epsilon_2 + 2\epsilon_1} \right), \tag{11}$$

where $\epsilon_1 = 1$ and $\epsilon_2 = 13$ and f is the concentration of the ϵ_2 material. As for the conventional CPA (or the effective medium theory), ϵ_e is given by solving the following equation:

$$\frac{3(1 - f)}{2 + \frac{\epsilon_1}{\epsilon_e}} + \frac{3f}{2 + \frac{\epsilon_2}{\epsilon_e}} = 1. \tag{12}$$

The agreement of the coated CPA with the fcc numerical results is clearly seen in Fig. 4 and this agreement is also consistent with a value of $z = 1.65$. Finally, we want to point out that all the theories agree between themselves as well as with the numerical results for low values of filling ratio f. This is expected, since the weak scattering limit theory and its CPA extensions coincide in the limit $f \to 0$ as can be seen by comparing Eq. (10) with Eq. (11).

As another check of the coated CPA, we present results for the experimental situation studied by the Amsterdam group.[8] Their experiments[8] involved the multiple scattering of light of wavelength $\lambda = 633$ nm from TiO_2 particles with average radius $R = 110$ nm, an index of refraction $\sqrt{\epsilon_2} = 2.73$ and a volume fraction of 36%. An accurate comparison[8] between time-resolved and steady-state measurements concluded that the transport mean free path was $\ell_t = 0.57 \pm 0.05$ μm so $k\ell_t \simeq 5.6$ and the diffusion speed of light, $v_E = (5 \pm 1)10^7$ m s^{-1} = $(0.17 \pm 0.03)c$. This is indeed a very small value for the effective velocity for the propagation of EM waves in random dielectric spheres. Their measured diffusion constant is $D = v_E \ell_t / 3 = 11.7$ m^2 s^{-1}. In Fig. 5(a), we present the results for the phase velocity [given by Eq. (9b)], the energy transport velocity, v_E, is given by Eqs. (28) and (29) of Ref. 8, and the coated CPA results for the effective phase velocity, v_{CPA}, and the CPA energy velocity v'_E. The CPA phase velocity is defined as ω/k [see Eq. (3)]. The CPA energy velocity, v'_E, is obtained by extending the Amsterdam group[8] approach for calculating v_E the following way. We are using the coated CPA to calculate a frequency-dependent effective dielectric function for each f. We then use the energy velocity expression of Lagendijk et al.[8] to calculate v'_E with the outside medium having our CPA effective dielectric function ϵ_e (which is frequency dependent) instead of $\epsilon_{outs} = 1$ as in the v_E calculation. This approach for low f gives a v'_E, which completely agrees with Lagendijk's formula (see Fig. 11) since ϵ_e is very close to unity for this case. As f increases ϵ_e gets larger than one and in addition develops
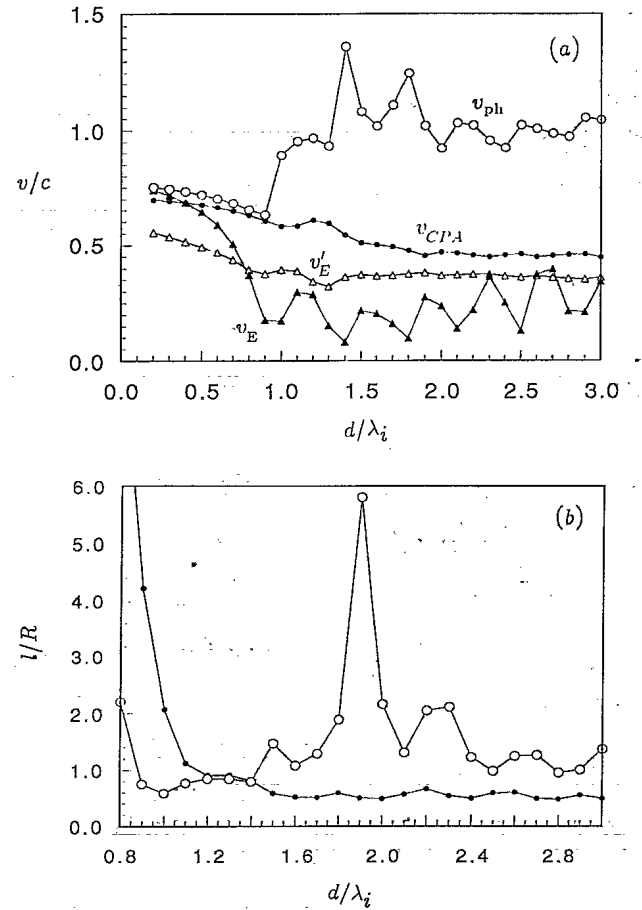

FIG. 5. (a) The phase velocity, v_{ph}, the energy transport velocity, v_E, the coated CPA effective phase velocity, v_{CPA}, and the CPA energy-transport velocity, v'_E, vs d/λ_i for $\sqrt{\epsilon_i} = 2.73$ dielectric spheres with filling ratio $f = 36\%$. d is the diameter of the sphere and $\lambda_i = 2\pi c/\omega\sqrt{\epsilon_i}$ is the wavelength inside the sphere. (b) The mean free path versus d/λ_i. The black circles give the results for ℓ within the coated CPA, while the white circles give the results within the low concentration limit theory.

some frequency dependence. For $f = 0.60$, v'_E calculated this way shows very little structure in agreement with experiment and our coated CPA velocity. We feel that this is a reasonable method to treat the difficult regime of transport properties in the high concentration limit as a function of d/λ_i, for the experimental situation described above. d is the diameter of the dielectric sphere and $\lambda_i = 2\pi c/\omega\sqrt{\epsilon_2}$ is the wavelength inside the sphere. We choose to present our results this way, since strong Mie resonances appear in the total scattering cross section from the isolated sphere and in the limit $\epsilon_2/\epsilon_1 \to \infty$, when $d/\lambda_i = (n+1)/2$, with $n = 1, 2, 3...$ for the vector case and $n = 0, 1, 2, 3, ...$ for the scalar case. Notice that both the phase velocity and the energy transport velocity give a lot of structure, especially close to the Mie resonances. This is expected because both of these quantities were calculated[8] within a theory valid for the low concentration limit, i.e., for just one isolated dielectric scatterer. It is expected that the omitted multiple scattering would smoothen out the strong fluctuations shown in Fig. 5(a).[8] The phase velocity calculated by the formulas given in Eqs. (6) and (9a), give unphysical values, i.e., $v_{\rm ph} > c$ especially close to the isolated Mie resonances. The energy-transport velocity v_E differs considerably from the phase velocity and is always lower than $v_{\rm ph}$, but has a lot of spurious structure due to its calculation procedures which are based on scattering from a single isolated scatterer. The coated CPA, which is a self-consistent approximation, gives results which do not show large fluctuations in either phase velocity ($v_{\rm CPA}$) or in the energy velocity (v'_E) as a function of d/λ_i. As seen in Fig. 5(a), the values of the CPA velocities are clearly lower than $v_{\rm ph}$ with the v'_E being lower and closer to v_E. In Fig. 5(b), we present the results of the mean free path ℓ normalized to the radius R of the dielectric spheres vs d/λ_i for the low concentration limit [see Eq. (8)] and for the coated CPA. Notice that the CPA mean free path does not have any strong structure for this case of 36% filling ratio, in contrast to the case of the low concentration based ℓ. For low values of d/λ_i, i.e., low values of ω both mean free paths behave as $1/\omega^4$, as expected from Rayleigh scattering. To compare our results with experiments[8] note that for $d/\lambda_i \approx 0.95$ we have from Fig. 5(a) that $v_E \approx 0.14c$ and $v'_E \approx 0.39c$ while the Amsterdam group's deduction for v_E is $(0.17 \pm 0.03)c$. The scattering mean free path ℓ according to our CPA is $\ell \approx 3R$ to be compared with a transport mean free path, ℓ_t, estimated experimentally[8] to be $(5.2 \pm 0.5)R$. Our theoretical value for the formula $D = \frac{1}{3}v'_E\ell$ equals 12.9 $m^2 s^{-1}$, in rather good agreement with the experimental value of 11.7 m^2 s^{-1}.

To further check the coated CPA we compare it with recent experiments of Genack and his collaborators.[17] In their first experiment, they have measured the frequency dependence of microwave propagation in a sample of 1/2-in. polystyrene spheres with index of refraction 1.59 and filling ratio of 56%. Their experimental results are presented in Fig. 6, where the frequency dependence of the diffusion constant, transport velocity, and mean free path are shown. The relation between the experimental frequency ν and d/λ_i is, in this case, $\nu({\rm GHz}) \simeq 15(d/\lambda_i)$.

Since the experiments were done in the frequency range of 18–24 GHz, this means d/λ_i is in the range from 1.2 to 1.8, which is around the second Mie resonance of the isolate sphere with index of refraction equal to 1.59 and radius $R = 0.64$ cm. In Fig. 7(a), we present the theoret-
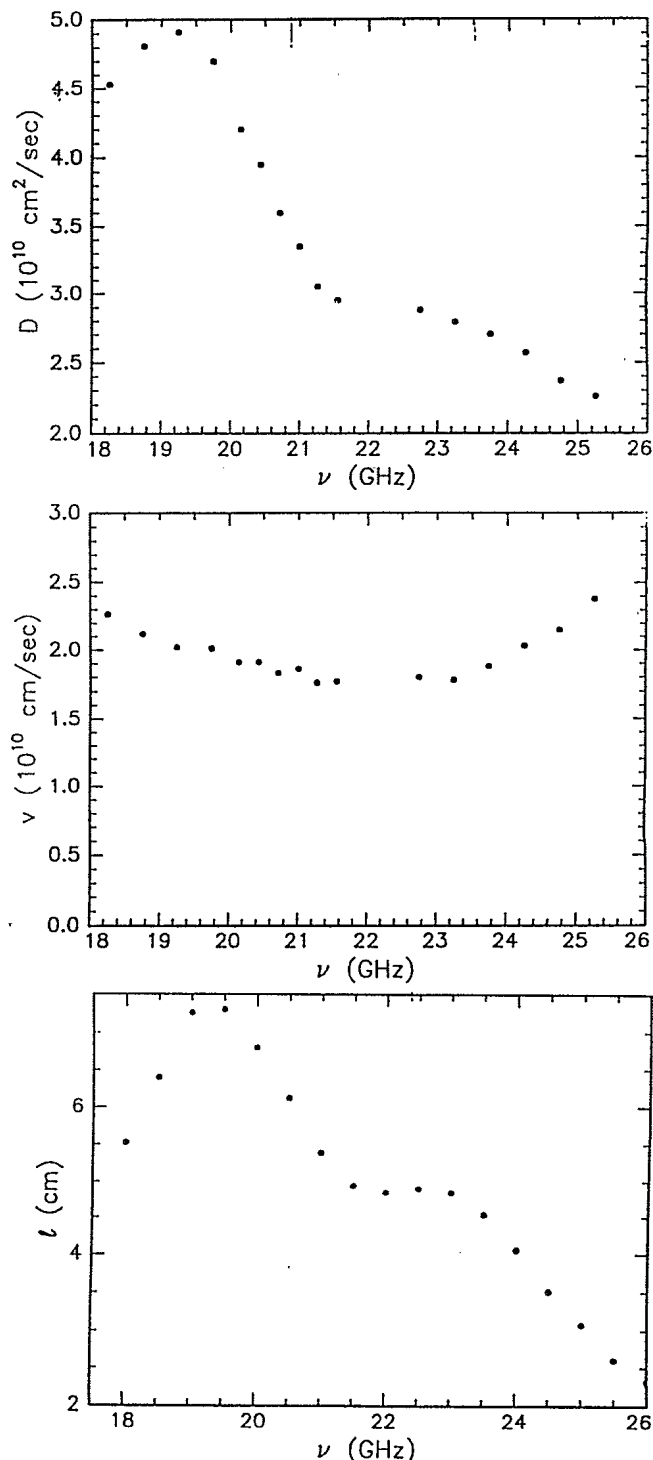

FIG. 6. The frequency dependence of the diffusion constant, transport velocity, and mean free path for a sample of 1/2-in. polystyrene spheres with index of refraction 1.59 and filling ratio of 59% [experiments by Genack et al. Ref. 17)].

ical results for the v_{ph}, v_E, v'_E, and v_{CPA} vs d/λ_i, while in Fig. 7(b), we present the results for the mean free path calculated within the coated CPA (solid spheres) and within the weak scattering limit. Notice in Fig. 7(a) that again v_E has relatively large structures close to the isolated Mie resonances, but not as strong as in the previous case of Fig. 5(a), since in this case the index of refraction for polystyrene is much lower. By comparing the experimental results for the transport velocity (Fig. 6) with the theoretical results (Fig. 7), one can clearly see that in this case the coated CPA, v'_E, gives results in rather good agreement with experiments. For the entire frequency range of 18–24 GHz (or equivalently d/λ_i=1.2–1.8), the experimental transport velocity does not have any strong structure and is roughly equal to $(0.6\text{–}0.8)c$ in agreement with the coated CPA v'_E, which is about $0.65c$. However, v'_E is flatter than the experimental one. As far as the comparison of the experimental mean free path Fig. 6 and the coated CPA path [Fig. 7(b)], there is indeed a semiquantitative agreement for $\nu \geq 19$ GHz (or $d/\lambda_i \geq 1.27$) but the experimental drop in low frequen-
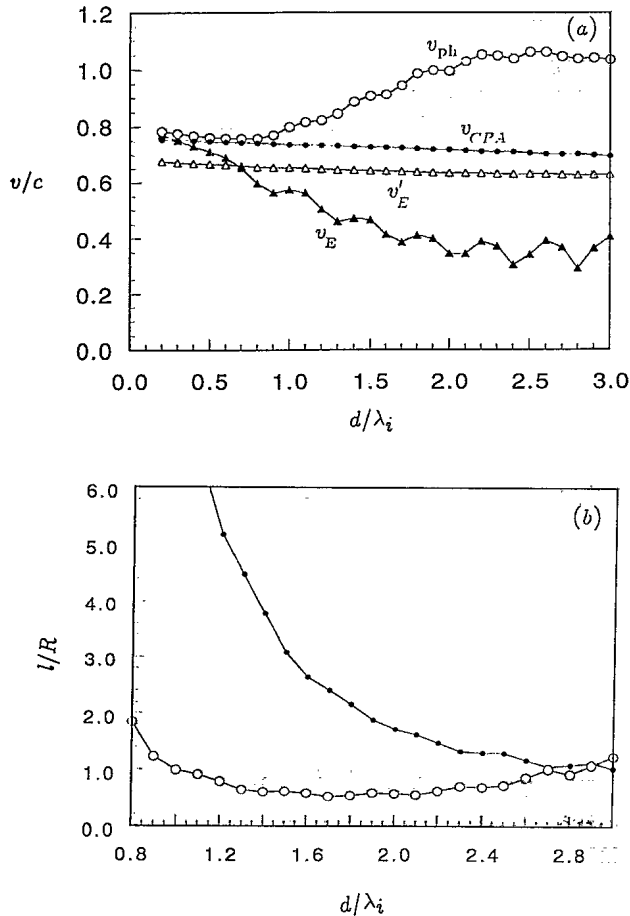
cies is very difficult to understand theoretically. A close examination of the experimental data for the mean free path shows that $\ell = 4R$ for d/λ_i=1.7 (or $\nu = 26$GHz) and monotonically increases to $\ell \simeq 11R$ at d/λ_i=1.27 (or ν=19 GHz). The corresponding theoretical results are $\ell \simeq 2.5R$ and $\ell \simeq 5R$ for the two frequencies, i.e., a factor of 2 lower than the experiment. We believe this discrepancy is due to the fact that the filling ratio is high ($f \simeq 0.56$), almost close packing and in this case we have strong short-range order. This order is responsible for the high values of ℓ in the experiment. While the coated CPA takes some of the short range into account, still it is an effective medium theory and does not have the capability of predicting that at filling ratios f close to the close packing ℓ might indeed become very large. To simulate this behavior, we multiplied the imaginary part of the self-energy by the factor $[1 - (f/0.64)]$ as we iterate the self-consistent equation [Eq. (4)] to derive the effective dielectric constant. This extra factor, by construction, gives that ℓ will go to infinity, i.e., we have extended states as we approach the random close packing of $f \simeq 64\%$. The results presented in Fig. 7(b) for ℓ within the coated CPA were calculated with this extra factor in. As we discussed before, there is indeed a quantitative discrepancy between theory and experiment, but the trend is similar.

In their second experiment,[17] Genack et al. measured the frequency dependence of microwave propagation in a sample of a mixture of nearly spherical, 3/8-in. solid alumina and hollow polypropylene spheres of the same diameter. The index of refraction of the solid alumina spheres is 3.0. By varying the volume fraction f of alumina spheres, it is possible to find the optimum values of f and frequency at which the strongest scattering occurs. Their experimental results are presented in Fig. 8, where the frequency dependence of the diffusion coefficient for various filling fractions f of alumina spheres is shown. The relation between the experimental fre-

FIG. 7. (a) The phase velocity, v_{ph}, the energy-transport velocity, v_E, the coated CPA effective phase velocity, v_{CPA}, and the CPA energy transport velocity, v'_E, vs d/λ_i for the polystyrene spheres of Fig. 6. (b) The mean free path vs d/λ_i. The black circles give the results for ℓ within the coated CPA while the white circles give the results within the low concentration limit theory.
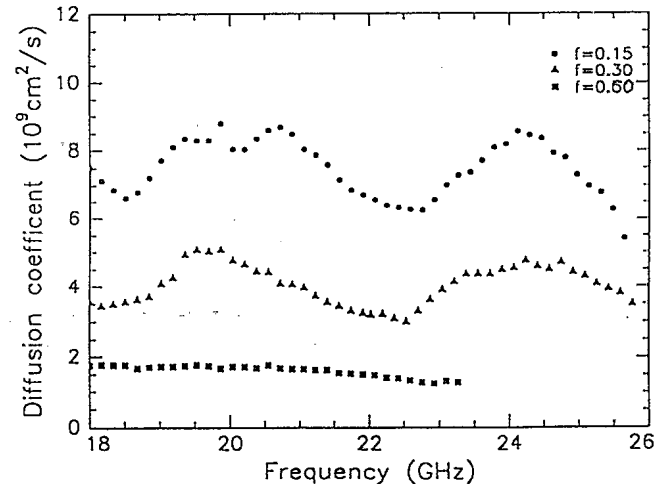

FIG. 8. The frequency dependence of the diffusion coefficient for mixtures of nearly spherical 3/8-in. solid alumina with index of refraction equal to 3.0 and hollow polypropylene spheres of the same diameter for different values of filling ratios [experiments by Genack et al. (Ref. 17)].

quency ν and d/λ_i is, in this case, $\nu(\text{GHz}) = 10(d/\lambda_i)$. Since the experiments were done in the frequency range of 18–24 GHz, this means that d/λ_i ranges from 1.8 to 2.6, which spans the region around the second and the third Mie resonances. Notice that the diffusion constant D has a strong frequency dependence for both $f = 0.15$ and $f = 0.30$. The maximum of D are very close to the Mie resonances of the isolated sphere, which are at 20 and 25 GHz. However, for $f = 0.60$, D is nearly independent of frequency, indicating the breakdown of the low concentration limit, which assumes that the dielectric scatterers are independent. In Fig. 9, we present the coated CPA results for the diffusion coefficient D. D was calculated using the formula $D = v'_E \ell/3$, where both v'_E and ℓ were calculated within the coated CPA theory. Notice that indeed the coated CPA results give results for D that agree only qualitatively with experiment. There is strong structure in D for $f = 0.15$, as expected from an independent scatterer model which is applicable for low f. As f increases, $f = 0.30$, there is also structure in D but by $f = 0.60$, there is almost no frequency dependence in D, for the experimental frequency range which spans from $d/\lambda_i = 1.8$ to 2.6.

In Fig. 10, we present the frequency dependence of the phase velocity, v_{CPA}, for various filling ratios f of alumina spheres calculated within the coated CPA. Notice there is strong structure in the v_{CPA} for $f = 0.15$ and values higher than c, while the CPA velocities for $f = 0.30$ and, in particular, for $f = 0.60$ show little or
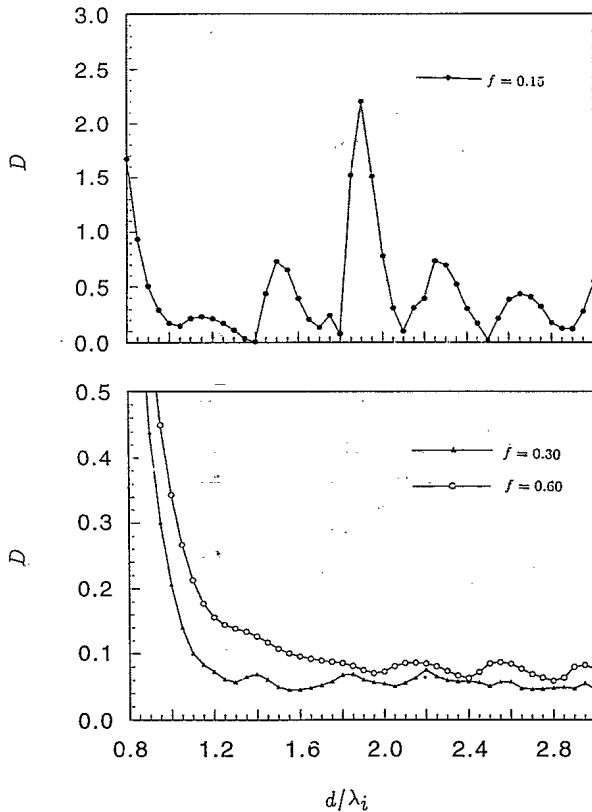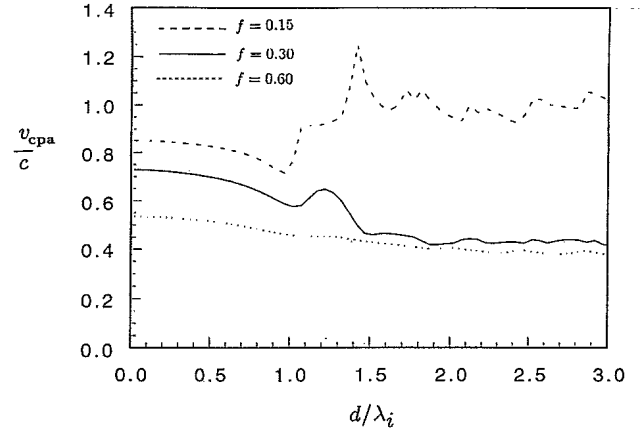

FIG. 10. The phase effective velocity, v_{CPA} calculated within the coated CPA vs d/λ_i for alumina spheres with index of refraction 3.0 for different values of filling ratios [experiments by Genack et al. (Ref. 17)].

no structure, as d/λ_i varies and v_{CPA} stays below c. We also present in Fig. 11, the frequency dependence of the energy-transport velocity, v_E,[8] for the three different filling ratios. Notice that the energy-transport velocity is always less than c, even for the case of $f = 0.15$ in contrast to the v_{CPA} result. In addition, there is very strong structure in v_E for all the filling ratios, and sometimes the value of v_E can be as low as $0.05c$. We want to point out again that the structure seen in the energy-transport velocity even for $f = 0.60$ is due to the independent scattering limit that was used in calculating v_E. Clearly the coated CPA does not have any of these limitations, especially for $f = 0.60$. For comparison we present in Fig. 12 results for our CPA extension of the energy-transport velocity, v'_E. We see that for low concentration ($f = 0.15$), v'_E almost coincides with v_E as expected. But for higher concentration, v'_E, while always remaining less than c is much smoother than v_E with values lower than v_{CPA} but on the average higher than v_E. It would be interesting to have additional careful measurements of the frequency dependence of the transport velocity for the 60% case of alumina spheres to see if there is any structure in the
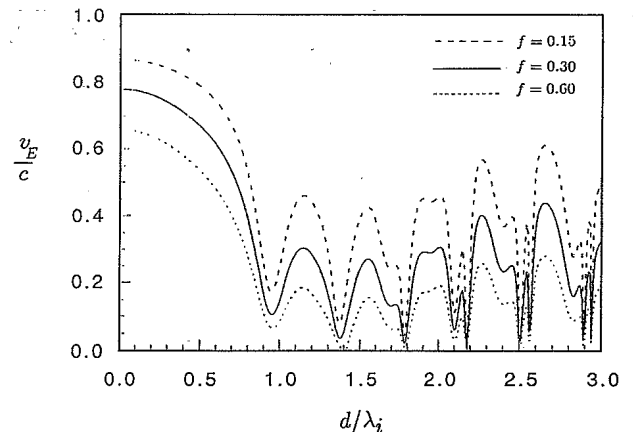

FIG. 9. The frequency dependence of the calculated, within the coated CPA, diffusion coefficients $D = \frac{1}{3}v'_E \ell$ for the alumina spheres described in Fig. 8.

FIG. 11. The energy-transport velocity (in the low concentration limit approximation), v_E, vs d/λ_i for alumina spheres with index of refraction 3.0 for different values of filling ratios.
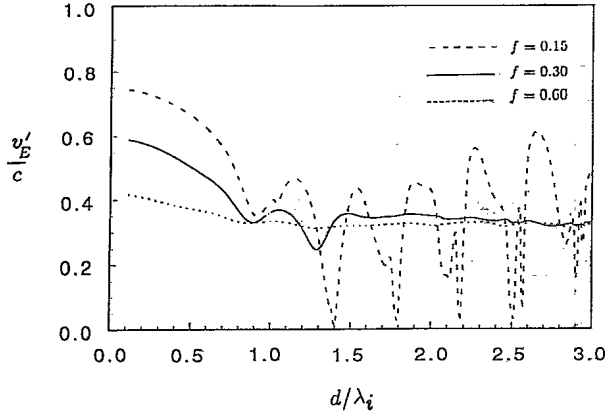
FIG. 12. The energy-transport velocity, v'_E (with the outside medium having the CPA effective dielectric constant which is frequency dependent and not equal to one) vs d/λ_i for alumina spheres with index of refraction 3.0 for different values of filling ratios.
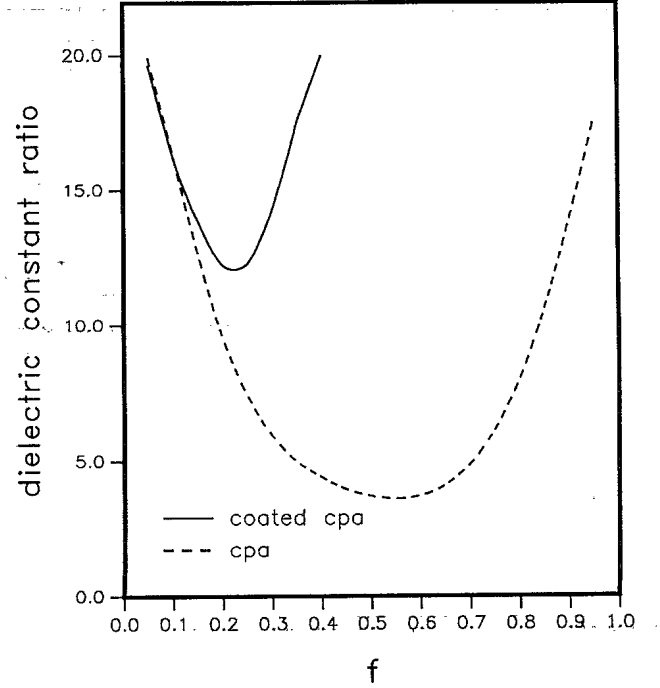

FIG. 13. The threshold value for the ratio ϵ_2/ϵ_1 for the appearance of localized states vs the filling ratio f for the EM case. The dotted line gives the coated CPA results, while the solid line gives the simple CPA results.

transport velocity.

As a final check of our coated CPA, we calculated the mobility edge trajectory for the scalar as well as the vector EM wave equation in 3D. In Fig. 13, we present the results for the vector case, where the threshold value of the dielectric constant ratio μ is shown as a function of f. Comparing Figs. 1(b) and 13, notice there is qualitative agreement between the positions of the band gaps [Fig. 1(b)] and the location of the mobility edge trajectory (Fig. 13). Probably the threshold value of ϵ_2/ϵ_1 is overestimated by the coated CPA at least for high f, in spite of the fact that for relatively low ϵ_2/ϵ_1 the value of ℓ is underestimated. We think the reason for this possible overestimation at large f is that the strong order induced in the system as the close-packing limit is approached is not properly incorporated in our CPA. As a result, the strong reduction in the density of states (which favors localization) is missing. On the other hand, the simple CPA, in spite of its complete omission of the short-range order, overestimates the randomness so strongly that may produce threshold values of ϵ_2/ϵ_1 close to reality for $0.5 \leq f \leq 0.7$. In conclusion, on the basis of the above arguments, we expect that the coated CPA is closer to reality for $f \leq 0.3$, while the simple CPA may be more realistic for $0.5 \leq f \leq 0.7$.

IV. CONCLUSIONS

In this paper we have presented an extension of the well-known CPA, where the basic scattering units are a coated sphere and a host material sphere embedded in an effective dielectric medium. This newly developed coated CPA takes into account some of the short-range order present in the random system under consideration, which is a random arrangement of dielectric spheres in a host background. Within our CPA, we have developed an extension of the Amsterdam group approach for calculating the energy-transport velocity. The validity of our approach is favorably tested by its agreement with

experimental results as well as with numerical calculations of the long-wavelength dielectric constant and the mobility edge trajectory. The results obtained, especially in the frequency regime where the wavelength is comparable to the size of the dielectric scattering units, show very interesting new behavior. The coated CPA is definitely an improvement over previous CPA's, but we want also to point out that it is also based on performing the average over only two scattering units. Therefore, its applicability in finding the mobility edge trajectories must be treated with caution. Possible improvements of our CPA may include a better choice of the R_s and R_v radii vs f and possibly some vertex corrections to the effective transport velocity v'_E and mean free path ℓ_t. The PWA used together with coated CPA in predicting the localization properties has been thoroughly tested only for electronic waves and its extension for classical, and especially EM, waves is a topic for further investigation.

[1] For a review see *Scattering and Localization of Classical Waves in Random Media*, edited by Ping Sheng (World Scientific, Singapore, 1990); *Photonic Band Gaps and Localization*, edited by C. M. Soukoulis (Plenum, New York, 1993). See also Philip St. J. Russel, Phys. World **37**, 37 (1992); S. John, Phys. Today **40**, 32 (1991).

[2] S. John, Phys. Rev. Lett. **53**, 2169 (1983); Phys. Rev. B **32**, 304 (1985); Comments Condens. Matter Phys. **14**, 193 (1988).

[3] C. M. Soukoulis, E. N. Economou, G. S. Grest, and M. H. Cohen, Phys. Rev. Lett. **62**, 575 (1989); E. N. Economou and C. M. Soukoulis, Phys. Rev. B **40**, 7977 (1989).

[4] Ping Sheng and Z. Q. Zhang, Phys. Rev. Lett. **57**, 1879 (1986).

[5] K. Arya, Z. B. Su, and J. L. Birman, Phys. Rev. Lett. **57**, 2725 (1986).

[6] C. A. Condat and T. R. Kirkpatrick, Phys. Rev. Lett. **58**, 226 (1987); Phys. Rev. B **32**, 495 (1985); T. R. Kirkpatrick, *ibid.* **31**, 5746 (1985).

[7] J. M. Drake and A. Z. Genack, Phys. Rev. Lett. **63**, 259 (1989); N. Garcia and A. Z. Genack, *ibid.* **66**, 1850 (1991); **66**, 2064 (1991).

[8] M. P. Albada, B. A. van Tiggelen, A. Lagendijk, and A. Tip, Phys. Rev. Lett. **66**, 3132 (1991); Phys. Rev. B 45, 12 233 (1992).

[9] Y. N. Barabanenkor and V. D. Ozrin, Phys. Rev. Lett. **69**, 1364 (1992).

[10] J. Kroha, C. M. Soukoulis, and P. Wölffe, Phys. Rev. B **47**, 11 093 (1993).

[11] E. N. Economou and A. D. Zdetsis, Phys. Rev. B **40**, 1334 (1989).

[12] E. N. Economou, C. M. Soukoulis, and A. D. Zdetsis, Phys. Rev. B **30**, 1686 (1984); see also E. N. Economou and C. M. Soukoulis (Ref. 1), p. 404.

[13] S. Datta, C. T. Chan, K. M. Ho, and C. M. Soukoulis, Phys. Rev. B **46**, 10 650 (1992).

[14] E. N. Economou and M. Sigalas, in *Photonic Band Gaps and Localization*, edited by C. M. Soukoulis (Plenum, New York, 1993), p. 317.

[15] C. F. Bohren and D. R. Huffman, *Absorption and Scattering of Light by Small Particles* (Wiley-Interscience, New York, 1983), p. 82 (single sphere), p. 181 (coated sphere), and p. 475 (computer programs).

[16] S. Datta, C. T. Chan, K. M. Ho, and C. M. Soukoulis, Phys. Rev. B **48**, 14 936 (1993).

[17] A. Z. Genack, J. H. Li, N. Garcia, and A. A. Lisyansky, in *Photonic Band Gaps and Localization*, edited by C. M. Soukoulis (Plenum, New York, 1993), p. 23.